Progress In Electromagnetics Research Letters, Vol. 94, 9–17, 2020

Decoupling of Dual-Band Microstrip Antenna Array with Hybrid Resonant Structure

Xin-Hong Li*

Abstract—A novel hybrid resonant structure is proposed to decouple a dual-band microstrip antenna array. The decoupling structure is composed of two H-shaped strips, and the lower and upper ones respectively collaborate with an X-shaped slot to reduce mutual coupling at 4.5 GHz and 5.5 GHz. Two sub-patches of different sizes share a connection feeding line to construct the dual-band array element, which is arranged along H-plane with the edge-to-edge spacing $0.15\lambda_l$ and $0.24\lambda_h$ (λ_l and λ_h are the free-space wavelengths of 4.5 GHz and 5.5 GHz, respectively). Simulated and measured results indicate that through loading the hybrid resonant structure, 31.6 dB and 24.0 dB reductions of mutual coupling at two frequencies are obtained, while the levels of coupling coefficients are both below -30 dB in two operating bands. Moreover, the modified radiation patterns, improved diversity metrics, and weakened coupled current distributions further verify its superior decoupling capability. The proposed decoupling structure reveals its promise in being employed in communication system and multielement linearly antenna arrays.

1. INTRODUCTION

Rapid advancement in wireless communication system calls for antenna arrays with superior performances, where mutual coupling is a crucial concern once densely arranging array elements, as it can result in a series of problems including mismatched impedance, deviated radiation pattern, enlarged side lobe, and scan blindness [1]. Also, the sizes of highly integrated devices are usually small due to limited space, but mutual coupling can merely be ignored when the distance between array elements is much larger than half wavelength. Meanwhile, to satisfy the demand of working in dual frequencies, dual-band antenna is often chosen as the basic element. Thus, it is of great significance to reduce mutual coupling of dual-band antenna array. Until now, various decoupling technologies have been presented and can be divided into three general categories. The first type is artificial electromagnetic material, which contains electromagnetic bandgap [2], frequency selective surface [3], metasurface [4, 5], defected ground structure [6–9], and array-antenna decoupling surface [10]. The second type is resonant structure [11, 12], which is employed to decouple antenna arrays at certain frequencies based on its resonant characteristic. The last one is to introduce a decoupling network [13, 14] to create extra currents to cancel out the coupled ones, and it is often adopted for dual-band cases [15–17]. However, most dual-band cases focus on decoupling monopole antenna arrays, and few hammer at microstrip antenna array. Also, researches on employing resonant structure for decoupling dual-band antenna arrays are scarcely reported.

In this research, a hybrid resonant structure, composed of an X-shaped slot and two H-shaped strips, is proposed to decouple dual-band microstrip antenna array at 4.5 GHz and 5.5 GHz. The array element combines two sub-patches of different sizes with a communal connection feeding line to generate two resonant frequencies. Then, the elements are arranged along H-plane, whose edge-to-edge distances

Received 30 July 2020, Accepted 4 September 2020, Scheduled 13 October 2020
* Corresponding author: Xin-Hong Li (ycu_lixh@163.com).
The author is with the School of Mathematics and Computer Science, Yichun University, Yichun, Jiangxi 336000, China.

are $0.15\lambda_l$ and $0.24\lambda_h$ at two frequencies. The lower H-shaped strip and the X-shaped slot work together to reduce mutual coupling at 4.5 GHz, while the upper one collaborates with the slot to function at 5.5 GHz. Finally, the results exhibit that mutual coupling at two frequencies is reduced by 31.6 dB and 24.0 dB, and the isolations are above 30 dB in the working bands. Also, the H-plane radiation patterns are modified, and the diversity metrics are improved. The current distributions further elucidate the operating mechanisms and decoupling capability.

2. MICROSTRIP ANTENNA ARRAY AND HYBRID RESONANT STRUCTURE DESIGN

2.1. Dual-Band Antenna Array

Figure 1 demonstrates the geometry and configuration of the proposed two-element dual-band microstrip antenna array. The array element consists of two sub-patches with different sizes and a connection line, which is fed by a coaxial probe. When the array works at 4.5 GHz, the large sub-patch with the size of $l_1 \times w_1$ plays a major role, so does the small one with the size of $l_2 \times w_2$ at 5.5 GHz. Thus, through concatenating them together with line w_3, the single antenna element can simultaneously operate at dual bands. The microstrip antenna array elements, printed on an FR4 substrate with the total size of $L_g \times W_g \times h$ and the relative permittivity of 4.3, are separated by the spacing d, making the edge-to-edge distances $0.15\lambda_l$ and $0.24\lambda_h$ at two frequencies, then the center-to-center distances are $0.45\lambda_l$ and $0.55\lambda_h$, indicating relatively strong mutual coupling between array elements especially at low frequency. After being optimized in the simulation software HFSS, the detailed dimensions of the dual-band antenna array are listed in Table 1. Fig. 3 plots the simulated S-parameters of the coupled dual-band antenna

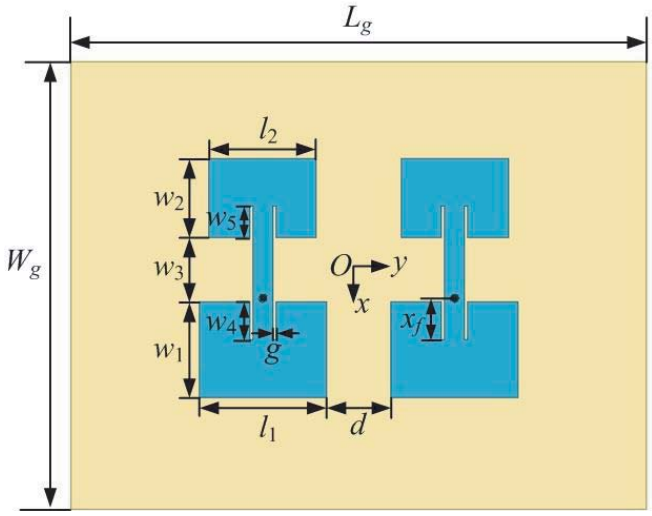

Figure 1. The geometry and configuration of the dual-band microstrip antenna array.

Table 1. Dimensions of the dual-band antenna array and hybrid decoupling resonant structure (Unit: mm).

L_g	W_g	h	l_1	l_2	x_f	g
90	70	1.5	20	16.8	6.5	0.5
w_1	w_2	w_3	w_4	w_5	d	s_1
15	12.5	10	6	5	10	5
s_2	s_3	s_4	s_5	s_6	s_7	s_8
6	1.5	4.5	9	2	60	8

array. It is apparent that the proposed antenna array resonates at two frequencies, and the coupling coefficients reach −14.6 dB and −19.6 dB at 4.5 GHz and 5.5 GHz, respectively.

2.2. Hybrid Decoupling Resonant Structure

It is conspicuous that a shorted microstrip line whose length is smaller than $\lambda_g/4$ (λ_g is the guided wavelength) usually acts as an inductor, while that with the length larger than $\lambda_g/4$ can behave as a combination of an inductor and a capacitor [18, 19]. Also, the slot can be deemed as a capacitor [20]. Therefore, by connecting two H-shaped strips and an X-shaped slot via four metallized holes, a novel hybrid decoupling resonant structure, displayed in Fig. 2, is proposed to reduce mutual coupling of the above dual-band antenna array. The length of the lower H-shaped strip is designed to be smaller than $\lambda_{gl}/4$ (λ_{gl} is the guided wavelength at 4.5 GHz) because of the limited space, while that of the upper one can be larger than $\lambda_{gh}/4$ (λ_{gh} is the guided wavelength at 5.5 GHz). Therefore, the low and high resonant frequencies, f_l and f_h, can be represented as

$$f_l = 1/2\pi\sqrt{L_l C}, \quad f_h = 1/2\pi\sqrt{L_h C C_h/\left(C + C_h\right)} \tag{1}$$

where L_l and L_h are the equivalent inductances of the lower and upper H-shaped strips, respectively, and C and C_h are the equivalent capacitances of the X-shaped slot and the upper H-shaped strips. Through changing the sizes of the lower strip and slot, f_l can be adjusted to the desired 4.5 GHz. Likewise, f_h can be fixed to 5.5 GHz when proper sizes of the upper strip and slot are selected. Based on the designing principle and optimization in HFSS, the dimensions of the hybrid decoupling resonant structure are ascertained in Table 1. From Fig. 3 which displays the simulated S-parameters of the decoupled antenna array, the hybrid decoupling resonant structure exhibits superior decoupling capability, as the coupling coefficients are reduced to −52.0 dB and −38.4 dB at two frequencies.

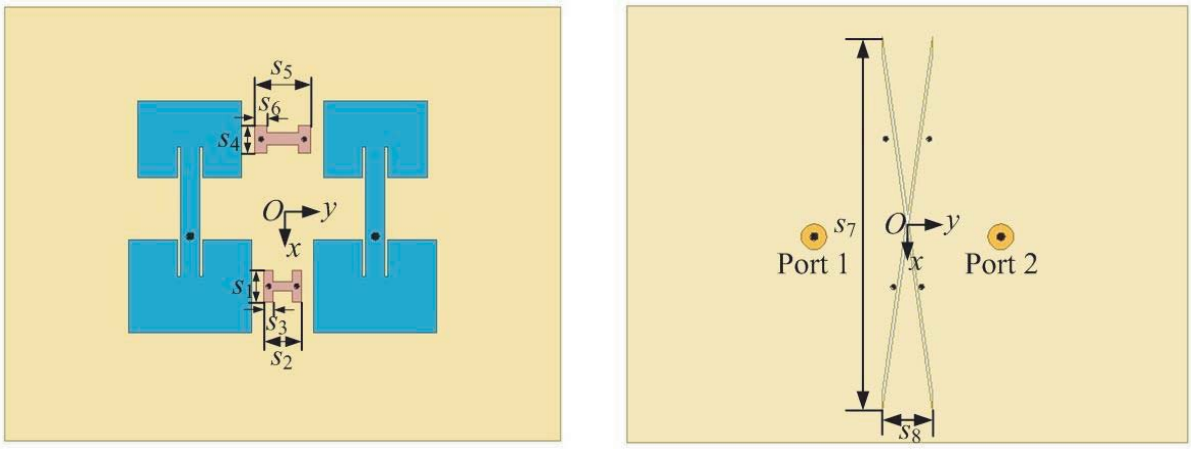

(a) (b)

Figure 2. The dual-band antenna array loaded with the hybrid decoupling resonant structure. (a) The top view; (b) The bottom view.

3. RESULTS AND DISCUSSION

To validate the effectiveness of the proposed hybrid decoupling resonant structure, the coupled and decoupled dual-band antenna arrays are fabricated, measured, and compared, whose prototypes are shown in Fig. 4.

3.1. *S*-Parameters

Figure 5 demonstrates the simulated and measured S-parameters of the two arrays, which indicate the good agreement with each other. The little discrepancy lies in the manufacturing and assembling errors.

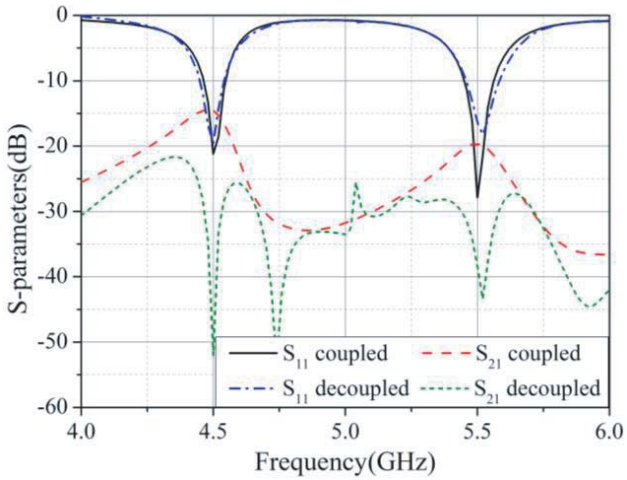

Figure 3. Simulated S-parameters of the coupled and decoupled dual-band antenna arrays.

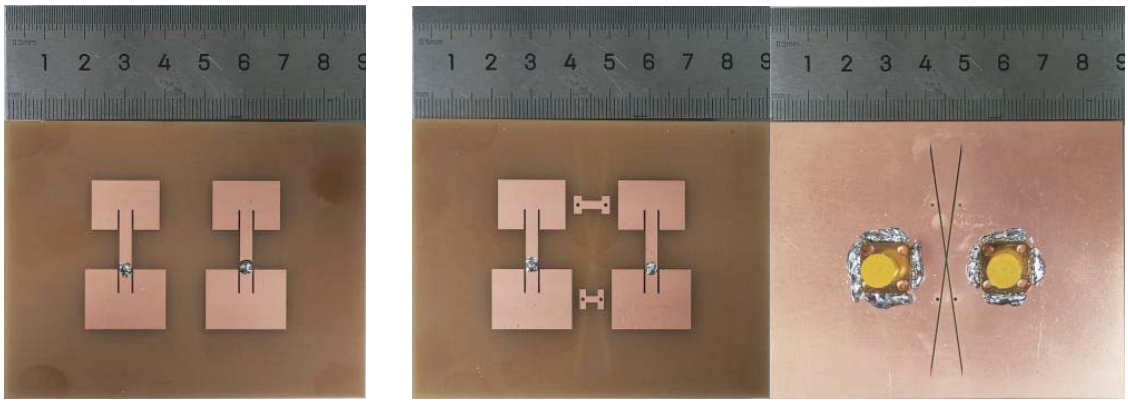

(a) (b)

Figure 4. The fabricated prototypes of the antenna arrays. (a) The coupled array; (b) The decoupled array.

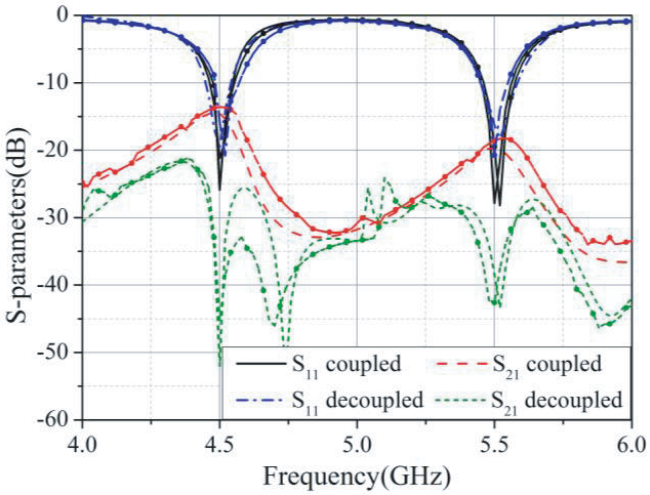

Figure 5. Simulated (line) and measured (line and symbol) S-parameters of the coupled and decoupled dual-band antenna arrays.

It is obvious that the two arrays are both well matched at designed frequencies. The simulated mutual coupling reductions are 37.4 dB and 18.8 dB. And at 4.5 GHz, the measured coupling coefficient drops from −13.6 dB to −45.2 dB, while at 5.5 GHz, the coefficient drops from −18.6 dB to −42.6 dB. That is to say, the measured coupling reductions are 31.6 dB and 24.0 dB, respectively. Meanwhile, in the two working bands, 4.48–4.58 GHz and 5.46–5.56 GHz, the levels of mutual coupling coefficients are both below −30 dB, which elucidates the superior decoupling capability of the proposed hybrid decoupling resonant structure.

3.2. Radiation Pattern and Gain

Figure 6 plots the simulated and measured radiation patterns of the two antenna arrays. It should be mentioned that during simulation or measurement, only port 1 is excited, while port 2 is terminated to a 50 Ω load. Usually, the strong mutual coupling between antenna elements can deteriorate the radiation patterns, especially in the arrangement direction. From Fig. 6(a), since the coupled dual-band antenna array is arranged in H-plane, the main direction of the H-plane radiation pattern deviates to 24° at 4.5 GHz. However, after the hybrid decoupling structure is loaded, the radiation pattern is modified to the broadside. Also, the simulated and measured gains respectively increase from 6.02 dBi and 5.73 dBi

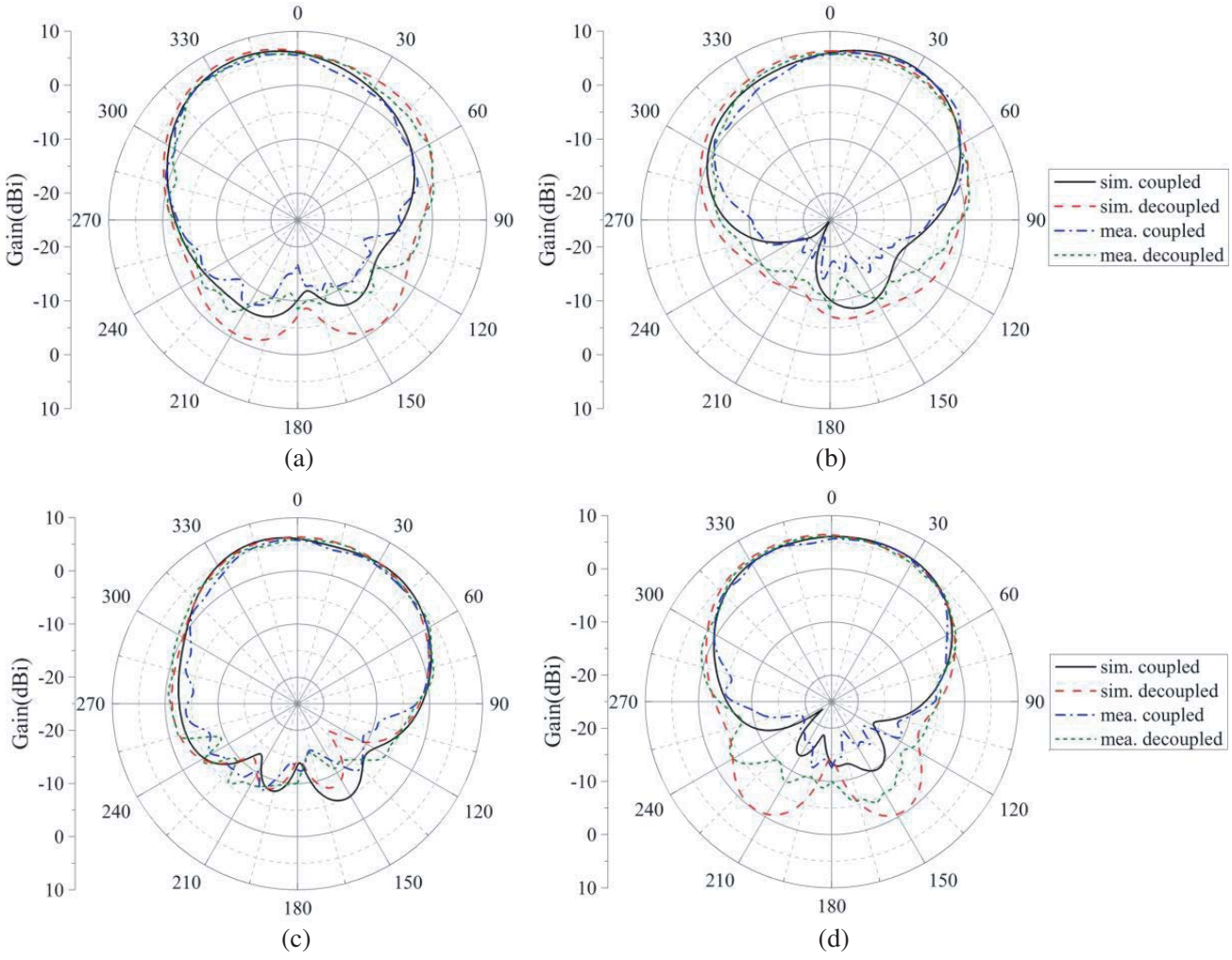

Figure 6. Simulated and measured radiation patterns of the coupled and decoupled dual-band antenna arrays with port 1 excited. (a) E-plane at 4.5 GHz; (b) H-plane at 4.5 GHz; (c) E-plane at 5.5 GHz; (d) H-plane at 5.5 GHz.

to 6.32 dBi and 5.96 dBi. Meanwhile, for the H-plane radiation pattern at 5.5 GHz, due to the relatively low mutual coupling, the coupled array can radiate to the broadside without any deflection, but the gain is a little improved. In detail, the simulated and measured gains respectively increase from 6.04 dBi and 5.82 dBi to 6.35 dBi and 6.17 dBi. Besides, the E-plane radiation patterns of the coupled and decoupled antenna arrays also deviate on account of the influence from relatively adjacent frequencies. On account of the asymmetry of the antenna element and array, the simulated and measured radiation patterns with two ports excited are also demonstrated in Fig. 7. The similar deviations exist in the E-plane radiation patterns, but the antenna array can radiate to the broadside in the H-plane. Moreover, the measured gains at 4.5 GHz and 5.5 GHz respectively increase from 8.32 dBi and 8.56 dBi to 8.97 dBi and 8.61 dBi. It is also evident that the backward radiation of the decoupled antenna array is enhanced, which exists in other references that adopt defected ground structures or slots [6–8] as decoupling structures, especially when the element spacing is small. However, compared to the superior decoupling capability of the hybrid decoupling structure, the drawbacks are inferior.

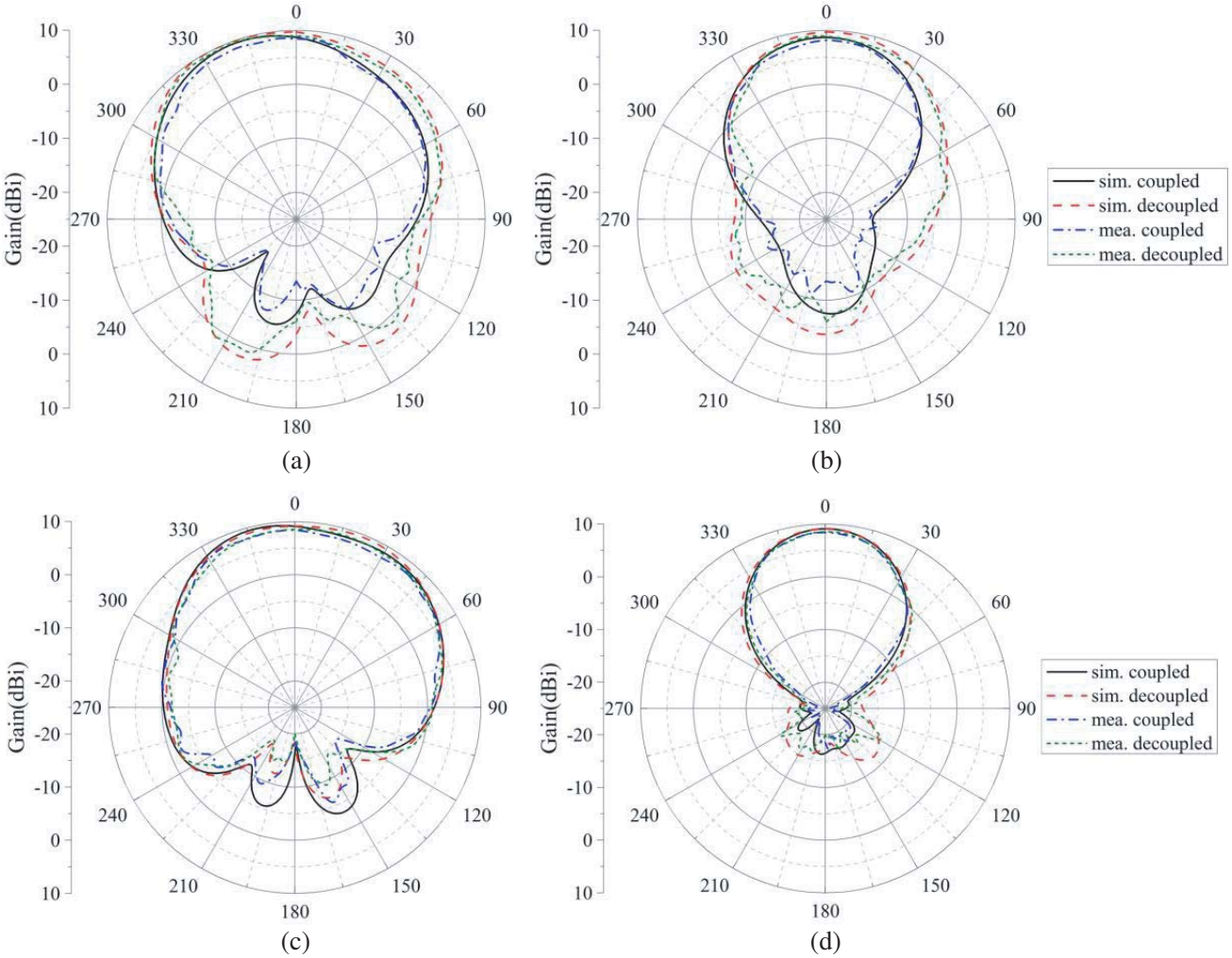

Figure 7. Simulated and measured radiation patterns of the coupled and decoupled dual-band antenna arrays with two ports excited. (a) E-plane at 4.5 GHz; (b) H-plane at 4.5 GHz; (c) E-plane at 5.5 GHz; (d) H-plane at 5.5 GHz.

3.3. Diversity Metrics

For a multiple input multiple output (MIMO) system, diversity metrics, including envelop correlation coefficient (ECC), diversity gain (DG), total active reflection coefficient (TARC), etc., are always significant parameters to evaluate its communication performance. ECC (ρ_e) is a typical parameter that can reveal the correlation of the antenna array elements, so is DG. They can be represented as [9]

$$\rho_e = \frac{\left|S_{11}^* S_{12} + S_{21}^* S_{22}\right|^2}{\left(1 - |S_{11}|^2 - |S_{21}|^2\right)\left(1 - |S_{22}|^2 - |S_{12}|^2\right)} \tag{2}$$

$$\mathrm{DG} = 10\sqrt{1 - \rho_e} \tag{3}$$

Usually, a minimized ECC and a maximized DG are required to maintain a high channel capacity and a good diversity performance [21]. Fig. 8(a) plots the measured calculated ECC and DG of the coupled and decoupled dual-band antenna arrays. It is apparent that the ECCs at 4.5 GHz and 5.5 GHz are decreased from 3.1×10^{-4} and 2×10^{-5} to 2×10^{-6} and 8.7×10^{-6}, which indicates a better diversity performance after decoupling.

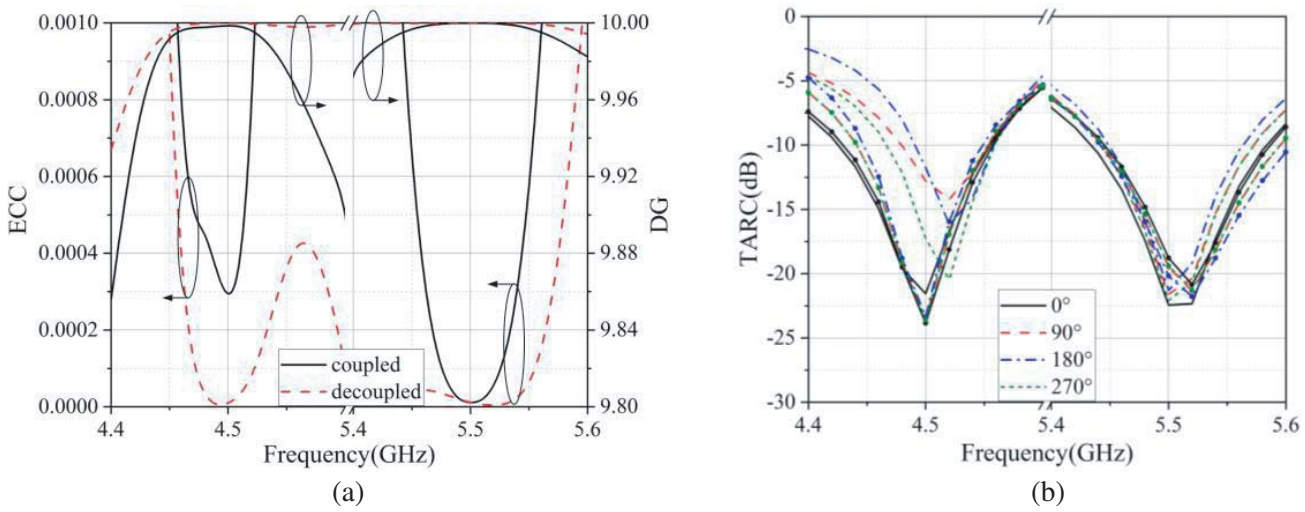

Figure 8. Diversity metrics of the coupled and decoupled dual-band antenna arrays. (a) ECC and DG; (b) TARC of the coupled (line) and decoupled (line and symbol) arrays.

One crucial index of the phased array is TARC, which takes the effect of the phases of the incoming signals into consideration. TARC is given by [22]

$$\Gamma_a^t = \sqrt{\frac{1}{2}\left(\left|S_{11} + S_{12}e^{j\theta}\right|^2 + \left|S_{21} + S_{22}e^{j\theta}\right|^2\right)} \tag{4}$$

where θ is the input feeding phase. Fig. 8(b) displays the measured TARC of the coupled and decoupled dual-band antenna arrays. At 4.5 GHz, TARC of the coupled array increases with θ varying, but that of the decoupled one remains below -20 dB. Meanwhile, the change of θ has little effect on TARCs at 5.5 GHz. Therefore, it is concluded that the hybrid decoupling structure can improve TARC and the scanning characteristic.

3.4. Current Distribution

To better intuitively understand the operating mechanisms of the dual-band antenna array and the hybrid decoupling resonant structure, the current distributions of the two antenna arrays are displayed in Fig. 9. Likewise, during simulation, port 1 is excited with port 2 connected to a 50 Ω load. From

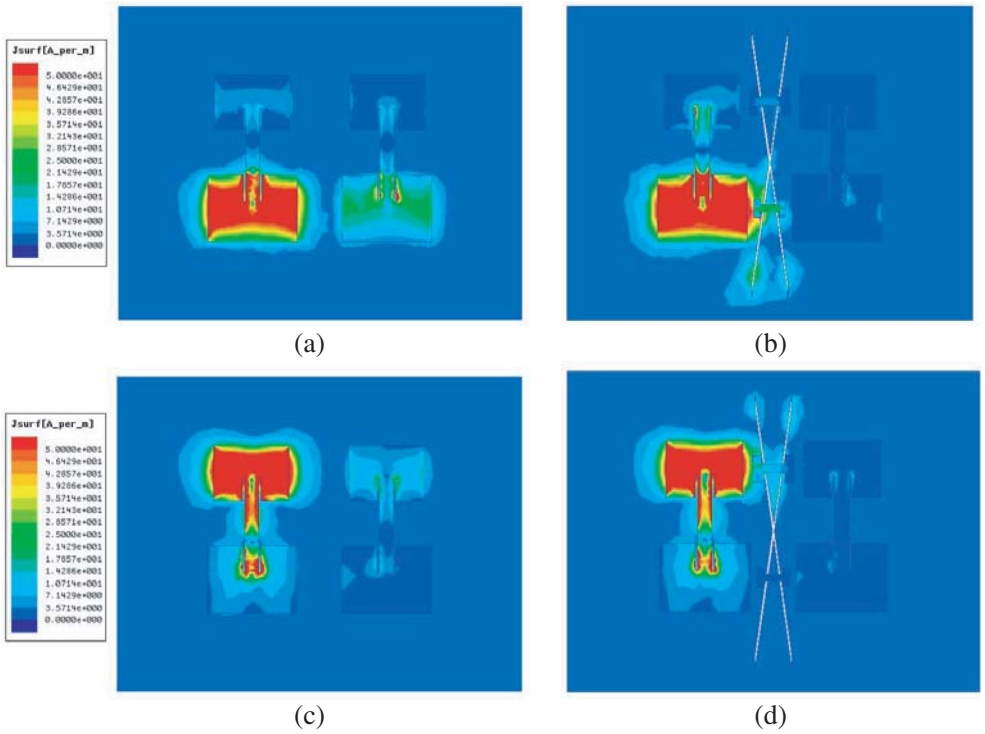

Figure 9. Current distributions of two antenna arrays. (a) The coupled array at 4.5 GHz; (b) The decoupled array at 4.5 GHz; (c) The coupled array at 5.5 GHz; (d) The decoupled array at 5.5 GHz.

Figs. 9(a) and (c), the working principle of the dual-band antenna array can be clarified. The large sub-patch dominates the radiation at 4.5 GHz, while the small one mainly works at 5.5 GHz. Besides, the mutual coupling between antenna elements is strong. But after adding the hybrid decoupling resonant structure, the currents coupled to the other patch are greatly weakened, which are evidently exhibited in Figs. 9(b) and (d). The lower H-shaped strip and X-shaped slot work together to obstruct the currents from flowing to the other patch at 4.5 GHz, while the upper strip and the slot collaborate to decouple the array at 5.5 GHz.

4. CONCLUSION

In this research, a novel hybrid decoupling resonant structure is presented to decouple a dual-band microstrip antenna array, whose element consists of two sub-patches and one connection feeding line. The lower and upper H-shaped strips respectively collaborate with the X-shaped slot to reduce mutual coupling at 4.5 GHz and 5.5 GHz. Simulated and measured results coincide with each other, revealing the superior decoupling capability of the proposed structure. 31.6 dB and 24.0 dB mutual coupling reductions are achieved, and the levels of coupling coefficients are both below -30 dB during the operating bands. Moreover, the H-plane radiation patterns are modified to the broadside, and the gains at two frequencies are improved. The results indicate that the proposed hybrid decoupling resonant structure has potential in the application of communication system and multielement linearly arrays.

REFERENCES

1. Allen, J. L. and B. L. Diamond, "Mutual coupling in array antennas," *Technical Report 424 (ESD-TR-66-443)*, Lincoln Laboratory, M.I.T., Lexington, MA, 1966.
2. Yang, F. and Y. Rahmat-Samii, "Microstrip antennas integrated with Electromagnetic Band-Gap (EBG) structures: A low mutual coupling design for array applications," *IEEE Transactions on Antennas and Propagation*, Vol. 51, No. 10, 2936–2946, 2003.

3. Zhu, Y., Y. Chen, and S. Yang, "Decoupling and low-profile design of dual-band dual-polarized base station antennas using frequency-selective surface," *IEEE Transactions on Antennas and Propagation*, Vol. 67, No. 8, 5272–5281, 2019.
4. Liu, F., J. Guo, L. Zhao, G.-L. Huang, Y. Li, and Y. Yin, "Dual-band metasurface-based decoupling method for two closely packed dual-band antennas," *IEEE Transactions on Antennas and Propagation*, Vol. 68, No. 1, 552–557, 2020.
5. Wang, Z., C. Li, and Y. Yin, "A Meta-surface Antenna Array Decoupling (MAAD) design to improve the isolation performance in a MIMO system," *IEEE Access*, Vol. 8, 61797–61805, 2020.
6. Abdel-Rahman, A. B., "Coupling reduction of antenna array elements using small interdigital capacitor loaded slots," *Progress In Electromagnetics Research C*, Vol. 27, 15–26, 2012.
7. Wei, K., J.-Y. Li, L. Wang, Z.-J. Xing, and R. Xu, "Mutual coupling reduction by novel fractal defected ground structure bandgap filter," *IEEE Transactions on Antennas and Propagation*, Vol. 64, No. 10, 4328–4335, 2016.
8. Han, X., H. Hafdallah Ouslimani, T. Zhang, and A. C. Priou, "CSRRs for efficient reduction of the electromagnetic interferences and mutual coupling in microstrip circuits," *Progress In Electromagnetics Research B*, Vol. 42, 291–309, 2012.
9. Fritz-Andrade, E., A. Perez-Miguel, R. Gomez-Villanueva, and H. Jardon-Aguilar, "Characteristic mode analysis applied to reduce the mutual coupling of a four-element patch MIMO antenna using a defected ground structure," *IET Microwaves, Antennas & Propagation*, Vol. 14, No. 2, 215–226, 2020.
10. Wu, K. L., C. Wei, X. Mei, and Z. Y. Zhang, "Array-antenna decoupling surface," *IEEE Transactions on Antennas and Propagation*, Vol. 65, No. 12, 6728–6738, 2017.
11. Alsath, M. G. N., M. Kanagasabai, and B. Balasubramanian, "Implementation of slotted meander-line resonators for isolation enhancement in microstrip patch antenna arrays," *IEEE Antennas and Wireless Propagation Letters*, Vol. 12, 15–18, 2013.
12. Maddio, S., G. Pelosi, M. Righini, S. Selleri, and I. Vecchi, "Mutual coupling reduction in multilayer patch antennas via meander line parasites," *Electronic Letters*, Vol. 54, No. 15, 922–924, 2018.
13. X.-J. Zou, G.-M. Wang, Y.-W. Wang, and H.-P. Li, "An efficient decoupling network between feeding points for multielement linear arrays," *IEEE Transactions on Antennas and Propagation*, Vol. 67, No. 5, 3101–3108, 2019.
14. Xia, R. L., S. W. Qu, P. F. Li, D. Q. Yang, S. Yang, and Z. P. Nie, "Wide-angle scanning phased array using an efficient decoupling network," *IEEE Transactions on Antennas and Propagation*, Vol. 63, No. 11, 5161–5165, 2015.
15. Albannay, M. M., J. C. Coetzee, X. Tang, and K. Mouthaan, "Dual-frequency decoupling for two distinct antennas," *IEEE Antennas and Wireless Propagation Letters*, Vol. 11, 1315–1318, 2012.
16. Ou, Y., X. Cai, and K. Qian, "Two-element compact antennas decoupled with a simple neutralization line," *Progress In Electromagnetics Research Letters*, Vol. 65, 63–68, 2017.
17. Zhao, L. and K.-L. Wu, "A dual-band coupled resonator decoupling network for two coupled antennas," *IEEE Transactions on Antennas and Propagation*, Vol. 63, No. 7, 2843–2850, 2015.
18. Hong, J. S., *Microstrip Filters for RF/Microwave Applications*, Wiley, New York, 2001.
19. Pozar, D. M., *Microwave Engineering*, 4th Edition, Wiley, New York, 2011.
20. Chiu, C. Y., C. H. Cheng, R. D. Murch, and C. R. Rowell, "Reduction of mutual coupling between closely-packed antenna elements," *IEEE Transactions on Antennas and Propagation*, Vol. 55, No. 6, 1732–1738, 2007.
21. Kildal, P. S. and K. Rosengren, "Correlation and capacity of MIMO systems and mutual coupling, radiation efficiency, and diversity gain of their antennas: Simulations and measurements in a reverberation chamber," *IEEE Communications Magazine*, Vol. 42, No. 12, 104–112, 2004.
22. Sharawi, M. S., "Printed multi-band MIMO antenna systems and their performance metrics," *IEEE Antennas and Propagation Magazine*, Vol. 55, No. 5, 218–232, 2013.